

# Effects of vibrational and rotational relaxation on the behavior of the $Q$ -branch profile of $\nu_1$ vibrations of $\text{CH}_4$ and $\text{SiH}_4$ molecules in dense gases

S. Yu. Volkov, D. N. Kozlov, M. R. Malikov, and V. V. Smirnov

*P. N. Lebedev Institute of Physics, Academy of Sciences of the USSR, Moscow*

(Submitted 2 June 1983)

Zh. Eksp. Teor Fiz. **86**, 826–834 (March 1984)

The results are presented of a study of the width and position of the  $Q$ -branch profile maximum for  $\nu_1$  vibrations of  $\text{CH}_4$  and  $\text{SiH}_4$  molecules. The measurements were performed with a resolution of  $0.001 \text{ cm}^{-1}$  at a density of 150 amagat and a temperature of 295 K, both in pure gases and in mixtures with argon. Contributions to the change in the shape of the profile due to vibrational and rotational relaxation were isolated, and the time constants and cross sections for these processes were determined.

1. Studies of line shapes in Raman spectra yield important information on intermolecular interactions and the associated vibrational and rotational relaxation processes in molecules. Particularly interesting from this point of view are studies of the  $Q$ -branch profile in isotropic Raman spectra due to vibrational-rotational transitions, since the dependence of these spectra on density is determined by both vibrational and rotational relaxation. The basic task in the analysis of such experimental data is to isolate the contribution of these relaxation processes to the change in the shape of the spectra. In this paper, we present the results of such an analysis, applied to measurements of the shape and width of the individual components as well as of the entire  $Q$ -branch profile of  $\nu_1$  vibrations of  $\text{CH}_4$  and  $\text{SiH}_4$  molecules as functions of pressure in the gaseous phase. The measurements were performed in a broad pressure range.

2. Most published work on line profiles in the Raman spectra of gases (see Ref. 1, pages 203–246 of Russ. transl.) has been confined to diatomic molecules for which many general properties of the isotropic  $Q$ -branch profile have been established as functions of density.

In tenuous gases, the  $Q$ -branch is split by the vibrational-rotational interactions into a series of individual  $J$ -components ( $J$  is the rotational quantum number). As the density  $N$  increases, the initial Doppler profile of these components is homogeneously and linearly broadened by rotationally inelastic collisions that alter the magnitude of the angular momentum  $\mathbf{J}$  and the rotational energy  $E$  of the molecules with characteristic relaxation times  $\tau_J$  and  $\tau_E$  (the width of the profile is  $\gamma_J \sim \tau_E^{-1} \sim N$ ). We note that collisions that alter the direction of the angular momentum do not effect the shape of the isotropic  $Q$ -branch profile.

When the broadening becomes comparable with the  $J$ -line splitting ( $\tau_E^{-1} \gtrsim 2\alpha \langle J \rangle$  where  $\alpha$  is the vibrational-rotational interaction constant), the  $Q$ -branch profile begins to be influenced by interference between contributions due to transitions from different  $J$ -states, the exchange between which is enhanced by the increase in collision frequency  $\tau_E^{-1}$ . As the density is increased still further, so that  $\tau_E^{-1} \gtrsim 2\pi c \delta_Q$  (where  $\delta_Q^2 = \langle (\nu - \nu_Q)^2 \rangle$  is the frequency variance in the spectrum and  $\nu_Q$  is the position of the "center of gravity" of the  $Q$ -branch with resolved structure), this interference leads to a smoothing, a symmetrization, and a narrowing of the  $Q$ -branch profile, and also to a nonlinear

shift of the frequency  $\nu^m$  of its maximum toward the centre of gravity by the amount  $\Delta_R$  from the vibrational frequency  $\nu_V$ . This phenomenon is called "collisional narrowing," and has now been investigated in detail both experimentally and theoretically (see, for example, Refs. 2–10). According to Refs. 7–9, at sufficiently high densities, for which  $(2\pi c \delta_Q \tau_E)^2 \ll 1$  and perturbation theory is valid, the central portion of the  $Q$ -branch has a Lorentz profile of width

$$\gamma_R = 4\pi c \delta_Q^2 \tau_E \sim N^{-1} \quad (1)$$

and the maximum is shifted by the amount  $\Delta_R = \nu_Q - \nu_V$ .

In addition to rotationally-inelastic collisions, the broadening  $\gamma_V$  and the shift  $\Delta_V$  of both the individual  $J$ -components and of the  $Q$ -branch profile as a whole contain contributions due to collisions that modify both the energy and phase of the vibrational states. The quantities  $\gamma_V$  and  $\Delta_V$  are then linear functions of density. Since the vibrational and rotational relaxation processes are statistically independent, their contributions to the width  $\gamma$  and frequency shift  $\nu^m$  of the  $Q$ -branch profile maximum are additive:

$$\gamma = \gamma_R + \gamma_V, \quad \nu^m = \nu_V + \Delta_R + \Delta_V. \quad (2)$$

For most diatomic molecules, the characteristic vibrational relaxation time is much greater than the rotational relaxation time. This can be used to investigate collisional narrowing of the  $Q$ -branch profile by rotationally-inelastic collisions which, in turn, provides a way of observing the broadening and shift due to vibrational relaxation as the density is increased further (up to a few hundred amagat). A similar situation may be regarded as characteristic for all the diatomic molecules that have been investigated.

The shape of the  $Q$ -branch profiles of polyatomic molecules can reflect their internal structure. Thus, firstly, the vibrational-rotational splitting of the  $Q$ -branches of complex molecules is appreciably smaller, and the number of rotational components is greater (due to the possible removal of degeneracy in the projection of the angular momentum  $J$ ), than in diatomic molecules. Secondly, the presence of a large number of vibrational states, and possible intramolecular interactions between them, enhance the effectiveness of vibrational relaxation. These effects provide us with grounds for supposing that, even at moderate densities, it is possible to observe in complex molecules the effective collisional narrowing and more clearly defined manifestations of vibration-

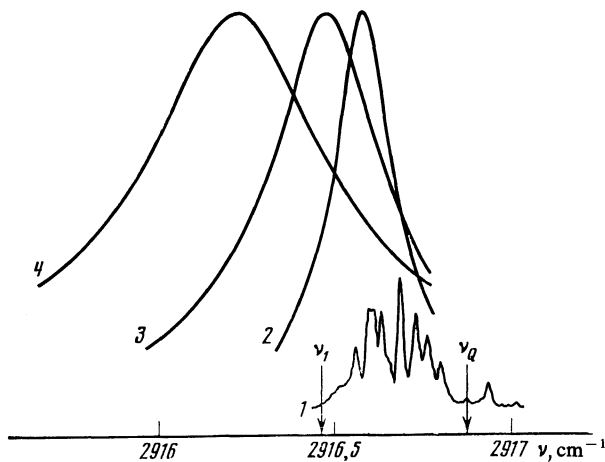


FIG. 1. Experimental CARS spectra of the  $Q_{01}$ -branch of the  $CH_4$  molecules at 295 K for different densities in pure gas (1,2) and in a mixture with argon (3,4): 1— $N_{CH_4} = 0.1$  amagat; 2— $N_{CH_4} = 5$  amagat; 3— $N_{Ar} = 35$  amagat; 4— $N_{Ar} = 85$  amagat.

al relaxation. Indeed, this can be seen in the data produced by the few measurements on polyatomic molecules performed so far, namely,  $N_2O$  (Refs. 11 and 12),  $CO_2$  (Ref. 13),  $C_2H_2$  (Ref. 14), and  $CH_4$  (Refs. 15–17). The absence of systematic studies of the line profiles of complex molecules in the gaseous phase is due to the limited spectral resolution and sensitivity of spontaneous Raman spectroscopy.

3. In recent years, the development of coherent Raman spectroscopy (Ref. 1, pp. 310–370, of the Russ. transl. and Ref. 18), capable of much higher sensitivity and spectral resolution, has made possible detailed studies of line shapes and frequencies of Raman-active transitions in polyatomic molecules in gases in a broad range of density. Even the early experiments exploiting these methods, and performed with a resolution of about  $0.001\text{ cm}^{-1}$ , yielded the  $Q$ -branch spectra of  $\nu_1$  vibrations of  $CH_4$  (Refs. 15 and 16) and  $\nu_2$  vibrations of  $C_2H_2$  (Ref. 14).

In the research reported here, coherent anti-Stokes Raman spectroscopy (CARS) was used to investigate the spectra of pure methane and silane (and also their mixtures with argon) at densities up to 150 amagat at room temperature ( $T = 295\text{ K}$ ). The spectra were recorded with the CARS spectrometer described in Ref. 19, using an instrumental resolution of about  $0.001\text{ cm}^{-1}$ . Some of the experimental  $Q_{01}$ -branch spectra of the  $CH_4$  molecule are shown in Fig. 1 for different densities.

In our previous papers<sup>20–23</sup> we reported studies of the structure of resolved  $Q_{01}$ -branch spectra of these molecules in low pressure gases. It was found that these spectra differed from the spectrum of a rigid spherical spinning top with its complex structure and a large number of closely spaced spectral lines. This was due to both the vibrational-rotational

interaction and the tetrahedral splitting of  $J$ -components into a definite, and  $J$ -dependent, number of lines. The resolved spectra were used to determine the quantities  $\nu_Q - \nu_1$  and  $\delta_Q$ . The results were, respectively,  $0.4\text{ cm}^{-1}$  and  $0.3\text{ cm}^{-1}$  for  $CH_4$ , and  $-2.2\text{ cm}^{-1}$  and  $1.8\text{ cm}^{-1}$  for  $SiH_4$ . We note that the frequencies of the  $Q_{01}$ -branch transitions in  $CH_4$  increase whereas in  $SiH_4$  they decrease with increasing  $J$ , so that the centers of gravity of these  $Q_{01}$ -branches lie on different sides of the vibrational frequency, and the quantities  $\Delta_R$  should have different signs.

The presence in  $CH_4$  and  $SiH_4$  of vibrational states ( $\nu_3$ ,  $2\nu_2$ ,  $2\nu_4$ , and  $\nu_2 + \nu_4$ ) close to  $\nu_1$  may favor an increase in the vibrational relaxation cross sections. The time for collisional transfer of vibrational excitation between some of these states was measured for  $CH_4$  in Ref. 24. The increase in the cross sections can also be due to intramolecular interactions of the  $\nu_1$  state (of the type of Fermi resonance with  $2\nu_2$  and  $2\nu_4$  in  $CH_4$  and the Coriolis resonance with  $\nu_3$  in  $SiH_4$ ), the presence of which is confirmed by data reported in Refs. 20–23 and 25.

The  $Q_{01}$ -branch spectra of  $CH_4$  and  $SiH_4$  with resolved structure were used to determine the widths  $\gamma_J$  of the individual rotational components with  $J = 2–5$  as functions of  $N$  in the range  $N = 0.01–0.4$  amagat. In this density range, collisional broadening appreciably exceeds the Doppler broadening, which is equal to  $0.006\text{ cm}^{-1}$  in  $SiH_4$  and  $0.011\text{ cm}^{-1}$  in  $CH_4$ . These data can be used to determine the linear expansion coefficients  $d\gamma_J/dN$ , and the relations

$$N\tau = (\pi c d\gamma/dN)^{-1}, \quad (3)$$

$$\sigma^\tau = \left[ 2 \left( \frac{2kT}{\pi\mu} \right)^{1/2} N_L \right]^{-1} \pi c \frac{d\gamma}{dN}, \quad (4)$$

can be used to find the corresponding relaxation rate constant  $N\tau(J)$  and the broadening cross sections  $\sigma_J^\tau$ , where  $N_L$  is the Loschmidt number and  $\mu$  is the reduced mass of the colliding particles. Table I lists the numerical values obtained in this way, together with the gas-kinetic collision cross sections  $\sigma_0$  for comparison.

For densities  $N \sim 0.4–1$  amagat, for which the spectral lines overlap, the changes in the shape of the  $Q_{01}$ -branch profiles are determined by the complex form of their rotational structure. It is important to note that, in this particular energy range, the collisional narrowing effect can appear only locally in the spectrum, because of the considerable irregularity in the disposition of the individual rotational components.

4. The behavior of the shape of the  $Q_{01}$ -branch profile of methane at high densities was studied both in the pure gas and in a mixture of methane and argon for different partial pressures of  $CH_4$ . For pure methane, and beginning with  $N \sim 1$  amagat, the  $Q_{01}$ -branch profile has a smooth form similar to the Lorentz shape, and its width  $\gamma$  and position  $\nu^m$  of

TABLE I.

Gas	$d\gamma_J/dN$ , $\text{cm}^{-1}\cdot\text{amagat}^{-1}$	$N\tau(J)$ , ns-amagat	$\sigma_J^\tau \cdot 10^{11}$ , $\text{cm}^2$	$\sigma_0 \cdot 10^{16}$ , $\text{cm}^2$
$CH_4$	$0.10 \pm 0.02$	$0.11 \pm 0.02$	$40 \pm 8$	54
$SiH_4$	$0.19 \pm 0.01$	$0.056 \pm 0.003$	$107 \pm 6$	$\sim 100$

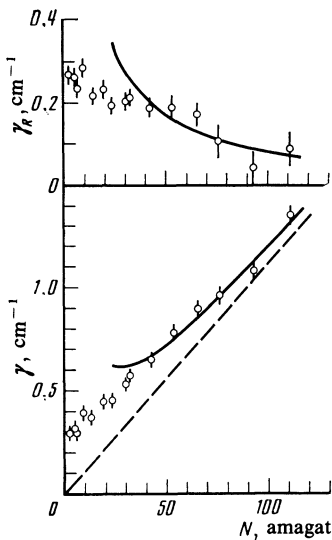


FIG. 2. CH<sub>4</sub>: density dependence of the Q<sub>01</sub>-branch linewidth and of the contribution due to rotational relaxation. Solid line—perturbation theory calculations, dashed line—contribution of  $\gamma_V$ .

its maximum in the pressure range 60–80 amagat vary nonlinearly with  $N$  (see Figs. 2 and 3). At higher densities,  $\gamma(N)$  and  $\nu^m(N)$  become linear functions, which indicates that vibrational relaxation plays a dominant role in changes in the Q<sub>01</sub>-branch profile or, according to (2), it indicates the validity of the relationships  $d\gamma/dN \simeq d\gamma_V/dN$ ,  $d\nu^m/dN \simeq d\Delta_V/dN$ . As a confirmation of this, we note that the coefficient of linear shift of the maximum, measured from the slope of the asymptote of the  $\nu^m(N)$  curve in Fig. 3, is  $-(1.73 \pm 0.03) \times 10^{-2} \text{ cm}^{-1} \text{ amagat}^{-1}$ , and remains constant up to

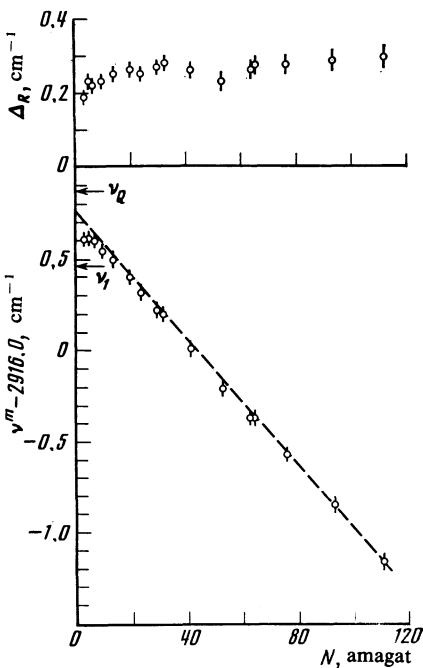


FIG. 3. CH<sub>4</sub>: density dependence of the frequency at maximum of the Q<sub>01</sub>-branch profile and of the contribution due to rotational relaxation. Dashed line—asymptotic behavior of the shift of the maximum at high densities.

high densities. This is shown by measurements in a gas for  $N \leq 400$  amagat ( $-1.72 \times 10^{-2} \text{ cm}^{-1} \text{ amagat}^{-1}$ ) (Ref. 26) and in a liquid ( $-1.73 \times 10^{-2} \text{ cm}^{-1} \text{ amagat}^{-1}$ ) (Ref. 27). The line shift cross section is given by

$$\sigma^{\Delta} = 2 \left[ 2 \left( \frac{2kT}{\pi\mu} \right)^{1/2} N_L \right]^{-1} \pi c \left| \frac{d\Delta}{dN} \right|, \quad (5)$$

and its numerical value is reproduced in Table II.

The nonlinearity of the functions  $\gamma(N)$  and  $\nu^m(N)$  is due to the collisional narrowing effect. This is confirmed by the following facts. Firstly, it is clear from the upper part of Fig. 3 that the nonlinear contributions  $\Delta_R(N)$  to the shift of the Q<sub>01</sub>-branch maximum, obtained by subtracting the linear vibrational shift  $\Delta_V = -1.73 \times 10^{-2} N \text{ cm}^{-1}$  from experimental values of  $\nu^m(N) - \nu_1$ , “saturates” for  $N \gtrsim 60$  amagat. The quantity  $\Delta_R$  reaches the value of  $0.3 \text{ cm}^{-1}$  in this region, which is roughly equal to the shift  $\nu\tau_Q - \nu_1 = 0.4 \text{ cm}^{-1}$  ( $\nu_1 = 2916.47 \text{ cm}^{-1}$ ). We note that collisions affecting vibrational and rotational motion lead in methane to a shift of the Q<sub>01</sub>-branch maximum in different directions. Secondly, the nonlinear contributions to the width of the Q<sub>01</sub>-branch also decrease appreciably with increasing density in the region  $N \leq 60$ –80 amagat, which should correspond to a narrowing of the profile in the absence of vibrational relaxation.

The slope of the experimental  $\gamma(N)$  curve in Fig. 2 can be used to estimate the vibrational broadening coefficient:  $d\gamma_V/dN \simeq 1.2 \times 10^{-2} \text{ cm}^{-1} \text{ amagat}^{-1}$ , which is lower by an order of magnitude than the broadening coefficient  $d\gamma_J/dN$  of the individual rotational components. This enables us to estimate the rotational relaxation time  $\tau_E$  on the assumption that  $\tau_E \simeq \tau(J)$ , and also to use the condition  $(2\pi c \gamma_Q \tau_E)^2 \ll 1$  to determine the density range ( $N > 6$  amagat) in which perturbation theory can be used to describe the behavior of the linewidth and to estimate the contributions of vibrational and rotational relaxation. The perturbation-theory results developed in Refs. 7–9 for the isotropic Q-branch of linear molecules [see (1) and (2)] will now be used in a further analysis of experimental data. The application of these results to spinning-top type molecules is founded on the assumption that differences between the structures of resolved Q-branches of molecules of different type have no effect on the overall behavior of the shape of the completely filled-in profile.<sup>9</sup>

According to (1) and (2), the function  $\gamma(N)$  can be written in the form

$$\gamma(N) = \gamma_R(N) + \gamma_V(N) = \frac{C_R}{N} + \frac{d\gamma_V}{dN} N, \quad (6)$$

where  $C_R = 4\pi c \delta_Q^2 \tau_E N$  is the rotational relaxation constant. Analysis of experimental data based on (6) for  $N \gtrsim 40$  amagat yields the following values for the coefficients:  $C_R = 8.3 \pm 0.3 \text{ cm}^{-1} \text{ amagat}$  and  $d\gamma_V/dN = (1.12 \pm 0.02) \times 10^{-2} \text{ cm}^{-1} \text{ amagat}^{-1}$ . The upper part of Fig. 2 shows the function  $\gamma_R(N)$  obtained by subtracting the vibrational contributions  $(d\gamma_V/dN)N$  from the experimental values of  $\gamma(N)$ . For comparison, we also show the  $\gamma_R = C_R/N$  curve predicted by perturbation theory. We note that, for densities  $N \leq 40$  amagat, the experimental function  $\gamma_R(N)$  is not monotonic but exhibits a number of small oscillations

TABLE II.

Gas	$(d\gamma_V/dN) \cdot 10^2$ , $\text{cm}^{-1} \cdot \text{amagat}^{-1}$	$N_V$ , ns·amagat	$\sigma_V^Y \cdot 10^{11}$ , $\text{cm}^2$	$N\tau_R$ , ns·amagat	$\sigma_R^Y \cdot 10^{11}$ , $\text{cm}^2$
CH <sub>4</sub>	1.12±0.02	0.95±0.02	4.4±0.1	0.12±0.03	36±8
CH <sub>4</sub> +Ar	0.80±0.03	1.33±0.05	3.8±0.1	—	—
SiH <sub>4</sub> +Ar	0.3	4	2	—	—

Gas	$(d\Delta_V/dN) \cdot 10^2$ , $\text{cm}^{-1} \cdot \text{amagat}^{-1}$	$\sigma_V^A \cdot 10^{11}$ , $\text{cm}^2$	$N\tau_E$ , ns·amagat	$\sigma_E \cdot 10^{11}$ , $\text{cm}^2$
CH <sub>4</sub>	-(1.73±0.03)	13.7±0.2	0.245±0.009	17±1
CH <sub>4</sub> +Ar	-(0.63±0.01)	6.0±0.1	0.245±0.009	20±1
SiH <sub>4</sub> +Ar	—	—	0.09	70

that can be related to the complex structure of the  $Q_{01}$ -branch.

We have used (3) and (4) to calculate the vibrational relaxation constant  $N\tau_V$  and the corresponding broadening cross section  $\sigma_V^Y$ . Assuming that the contribution to the width  $\gamma_J$  of the individual components of the  $Q_{01}$ -branch that is due to vibrational relaxation is determined by the quantity  $(d\gamma_V/dN)N$ , and eliminating it, we obtain the rotational relaxation constant  $N\tau$  and the cross section  $\sigma_V^R$  for the broadening of the individual  $J$ -components by rotational inelastic collisions (Table II).

At the same time, knowing  $C_R$ , we can use (1) to calculate the constant  $N\tau_E$  for the rate of relaxation of rotational energy, and the corresponding cross section  $\sigma_E$ . The values of these quantities are also listed in Table II. We note that the resulting values of the rotational relaxation constants  $N\tau_E$  and  $N\tau_R$  differ by a factor of 2. This difference may be due to the fact that  $N\tau_R$  characterizes the changes in rotational angular momentum produced by collisions, and the scale of these changes is determined by the strength of the collisions, whereas  $N\tau_E$  characterizes the evolution of the Boltzmann equilibrium over the entire ensemble of  $J$ -states.

When methane is diluted with argon (the density of  $N_{\text{CH}_4}$  was 5, 19, and 30 amagat), it is also possible to isolate contributions to the width  $\gamma$  of the  $Q_{01}$ -branch profile that are due to rotational and vibrational relaxation resulting from CH<sub>4</sub>-Ar collisions. For the quantitative analysis of experimental data on  $\gamma(N_{\text{CH}_4}, N_{\text{Ar}})$  (Fig. 4), we use an expression such as (6) which is obtained if we recall that  $\gamma_R \sim \tau_E$ ,  $\gamma_V \sim \tau V^{-1}$ , and the corresponding vibrational and rotational relaxation times are determined by

$$\tau^{-1} = \tau^{-1}(\text{CH}_4) + \tau^{-1}(\text{CH}_4\text{-Ar}), \quad (7)$$

where  $\tau^{-1}(\text{CH}_4) \sim N_{\text{CH}_4}$  and  $\tau^{-1}(\text{CH}_4\text{-Ar}) \sim N_{\text{Ar}}$  are the CH<sub>4</sub>-CH<sub>4</sub> and CH<sub>4</sub>-Ar collision frequencies. We have used (3), (4), (6), and (7) to calculate the quantities  $d\gamma/dN_{\text{Ar}}$ ,  $N_{\text{Ar}}\tau_E(\text{CH}_4\text{-Ar})$ ,  $N_{\text{Ar}}\tau_V(\text{CH}_4\text{-Ar})$ ,  $\sigma_E(\text{CH}_4\text{-Ar})$ , and  $\sigma_V^Y(\text{CH}_4\text{-Ar})$ . These are also listed in Table II.

For the same densities  $N_{\text{CH}_4}$  we measured  $\nu^m$  as a function of  $N_{\text{Ar}}$ . It is clear from Fig. 4 that this is a nonlinear function for low dilutions, but becomes linear for  $N_{\text{Ar}} \gtrsim N_{\text{CH}_4}$ , and the slope is the same for all the curves. This slope determines the magnitude of the vibrational shift coefficient  $d\Delta_V/dN_{\text{Ar}}$  or, according to (5), the cross sections  $\sigma_V^A(\text{CH}_4\text{-Ar})$  (see Table II). The observed nonlinearity of the shift in argon is independent, to within experimental error,

of the initial density  $N_{\text{CH}_4}$ , and is a function of only the ratio  $N_{\text{Ar}}/N_{\text{CH}_4}$ , so that

$$\nu^m(N_{\text{CH}_4}, N_{\text{Ar}}) - \nu^m(N_{\text{CH}_4}) = K(N_{\text{Ar}}/N_{\text{CH}_4})N_{\text{Ar}},$$

where  $K \simeq \text{const} = d\Delta_V/dN_{\text{Ar}}$  for  $N_{\text{Ar}}/N_{\text{CH}_4} \gg 1$  (see Fig. 5) and occurs for  $N_{\text{CH}_4}$  densities for which, in pure methane, the nonlinear contribution to the shift  $\Delta_R$  has already saturated. It may be concluded that, when methane is diluted with argon, the nonlinear shift of the  $Q_{01}$ -branch maximum is due to the shift of the vibrational frequency  $\nu_1$ . At the same time, the change in  $\nu_1$  of the methane molecules becomes sensitive to the presence of argon when its density exceeds the density of methane.

5. The behavior of the shape of the  $Q_{01}$ -branch of silane at high densities (up to 150 amagat) was investigated for a mixture of silane and a buffer gas (argon). The  $N_{\text{SiH}_4}$  density was 1 amagat. It is important to note that, for high relative densities of  $N_{\text{Ar}}/N_{\text{SiH}_4}$ , the experimental CARS spectra are distorted by interference between cubic nonlinear suscepti-

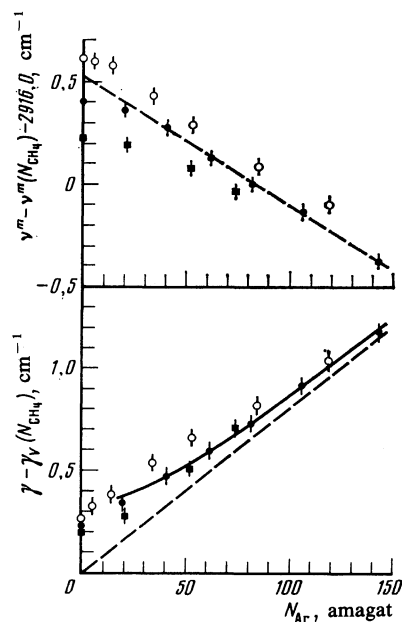


FIG. 4. CH<sub>4</sub> in Ar: broadening and shift of the frequency at maximum of the  $Q_{01}$ -branch profile as functions of the density  $N_{\text{Ar}}$ : ○— $N_{\text{CH}_4} = 5$  amagat, ●— $N_{\text{CH}_4} = 19$  amagat, ■— $N_{\text{CH}_4} = 30$  amagat. Solid line—perturbation theory calculations, dashed line—contribution of  $\gamma_V$  (bottom) and asymptotic behavior of the shift of the maximum for high  $N_{\text{Ar}}$  ( $N_{\text{CH}_4} = 19$  amagat).

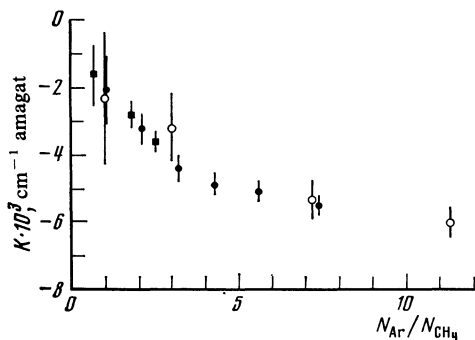


FIG. 5.  $\text{CH}_4$  in Ar: the shift function  $[v^m(N_{\text{CH}_4}, N_{\text{Ar}}) - v^m(N_{\text{CH}_4})]/N_{\text{Ar}}$  for the  $Q_{01}$ -branch profile maximum plotted against the gas density ratio:  $\circ$ — $N_{\text{CH}_4} = 5$  amagat,  $\bullet$ — $N_{\text{CH}_4} = 19$  amagat,  $\blacksquare$ — $N_{\text{CH}_4} = 30$  amagat.

bilities, i.e., the resonance susceptibility of the  $\text{SiH}_4$  molecules and the nonresonance susceptibility of the Ar atoms (Ref. 1, pp 310–370 of Russ. original and Ref. 18). The profile widths and the frequencies at maximum shown in Fig. 6, were obtained by analyzing experimental spectra with allowance for this effect.

For  $N_{\text{Ar}}$  densities in the range  $\sim 0$ –40 amagat, the profile is finally filled in, and the original  $Q_{01}$ -branch of  $\text{SiH}_4$  undergoes symmetrization at  $N_{\text{SiH}_4} = 1$  amagat, so that for  $N_{\text{Ar}} \gtrsim 40$  amagat, the shape of the  $Q_{01}$ -branch is nearly Lorentzian. As  $N_{\text{Ar}}$  increases, the profile width also increases, reaching a maximum for  $N_{\text{Ar}} \simeq 25$  amagat. Thereafter, for  $N_{\text{Ar}} \sim 25$ –80 amagat, the width decreases, but the profile begins to broaden again at high densities (Fig. 6). The maximum shifts towards lower frequencies in the direction of the center of gravity (which is separated by the amount  $\nu_Q - \nu_1 = -2.2 \text{ cm}^{-1}$  from the frequency  $\nu_1 = 2186.87 \text{ cm}^{-1}$ ), and the rate of shift decreases monotonically with increasing density.

The measured functions  $\gamma(N_{\text{Ar}})$  and  $\nu^m(N_{\text{Ar}})$  for silane in argon show evidence of both the collisional narrowing effect and vibrational relaxation. The characteristic feature of the spectral manifestation of collisional narrowing is the presence of a maximum on the function  $\gamma(N)$  in the CARS spectrum which, according to Ref. 8, should occur for densi-

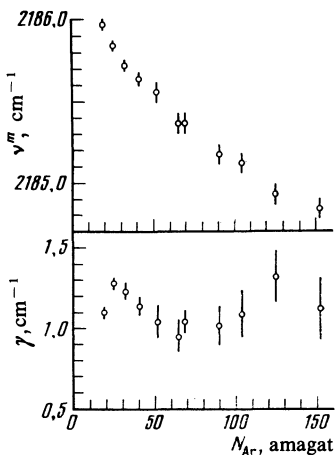


FIG. 6.  $\text{SiH}_4$  in Ar: width and frequency at maximum of the  $Q_{01}$ -branch profile as functions of  $N_{\text{Ar}}$  ( $N_{\text{SiH}_4} = 1$  amagat).

ties for which  $\Gamma = (2\pi c \delta_Q \tau_J)^{-1} = 0.5$ . In the experimental spectra, this maximum occurs at  $N_{\text{Ar}} \simeq 25$  amagat. By comparing the dimensionless parameter  $\Gamma$  with the densities  $N_{\text{Ar}}$  in the corresponding theoretical and experimental widths and profile shifts, we can show that  $N_{\text{Ar}} \tau_J(\text{SiH}_4\text{-Ar}) \simeq 0.17$  ns-amagat, and that the experimental data were obtained for densities  $N_{\text{Ar}}$  that corresponded to the “beginning” of collisional narrowing ( $\Gamma \lesssim 3$ ). Analysis of experimental data within the framework of perturbation theory (which is valid for  $\Gamma^2 \gg 1$ ) for densities satisfying this condition, yields the following estimated values of the coefficients  $C_R$  and  $d\gamma_V/dN_{\text{Ar}}$  [see (6)]:  $C_R \simeq 87 \text{ cm}^{-1}$  amagat and  $d\gamma_V/dN_{\text{Ar}} \simeq 0.003 \text{ cm}^{-1}$  amagat $^{-1}$ . From (1), (3), and (4) we then obtain the values of  $N_{\text{Ar}} \tau_E(\text{SiH}_4\text{-Ar})$ ,  $N_{\text{Ar}} \tau_V(\text{SiH}_4\text{-Ar})$ ,  $\sigma_E(\text{SiH}_4\text{-Ar})$ , and  $\sigma_V(\text{SiH}_4\text{-Ar})$  (see Table II).

6. Thus, our studies of the behavior of the  $Q_{01}$ -branch profile of  $\text{CH}_4$  and  $\text{SiH}_4$  molecules have shown that the spectral manifestations of the rotational relaxation of these polyatomic molecules and the linear molecules appear to be qualitatively similar, and have cross sections of the order of the gas-kinetic values. At the same time, the polyatomic molecules that were investigated exhibit an appreciable increase in the vibrational relaxation cross sections.

We have shown that the use of high-resolution coherent Raman spectroscopy has enabled us to follow the details of the qualitative changes in the shape and shift of line profiles at both low and high gas pressures. This approach ensures experimental precision that is sufficient to yield quantitative data on rotational and vibrational relaxation times of complex molecules.

The authors are greatly indebted to V. A. Alekseev and S. I. Temkin for fruitful discussions of the results and also to S. I. Mednikov for assistance in the numerical processing of the experimental data.

<sup>1</sup>A. Weber (ed.), Raman Spectroscopy of Liquids and Gases, Springer, 1979 [Russian translation ed. by I. L. Fabelinskii, Mir, Moscow, 1982].

<sup>2</sup>G. V. Mikhaïlov, Trudy, FIAN, 27, 150 (1964).

<sup>3</sup>V. A. Alekseev and I. I. Sobel'man, Zh. Eksp. Teor. Fiz. 55, 1974 (1968) [Sov. Phys. JETP 28, 991 (1969)].

<sup>4</sup>A. D. May, J. C. Stryland, and G. Varghese, Can. J. Phys. 48, 2331 (1970).

<sup>5</sup>P. Dion and A. D. May, Can. J. Phys. 51, 36 (1973).

<sup>6</sup>Y. Le Duff and W. J. Holzer, J. Chem. Phys. 60, 2175 (1974).

<sup>7</sup>A. I. Burshtein and S. I. Temkin, Zh. Eksp. Teor. Fiz. 71, 938 (1976) [Sov. Phys. JETP 44, 492 (1976)].

<sup>8</sup>S. I. Temkin and A. I. Burshtein, Pis'ma Zh. Eksp. Teor. Fiz. 28, 583 (1978) [JETP Lett. 28, 538 (1978)].

<sup>9</sup>A. I. Burshtein and S. I. Temkin, Spektroskopiya molekulyarnogo vrashcheniya v gasakh i zhidkostyakh (Spectroscopy of Molecular Rotation in Gases and Liquids), Nauka, Novosibirsk, 1982.

<sup>10</sup>V. A. Alekseev and A. V. Malyugin, Zh. Eksp. Teor. Fiz. 80, 897 (1981) [Sov. Phys. JETP 53, 456 (1981)].

<sup>11</sup>R. Ouillon, Chem. Phys. Lett. 35, 63 (1975).

<sup>12</sup>N. D. Orlova and L. A. Platonova, Opt. Spektrosk. 51, 746 (1981) [Opt. Spectrosc. (USSR) 51, 414 (1981)].

<sup>13</sup>P. A. Bazhulin and Yu. A. Lazarev, Opt. Spektrosk. 8, 206 (1960).

<sup>14</sup>V. V. Smirnov and V. I. Fabelinskii, Pis'ma Zh. Eksp. Teor. Fiz. 27, 131 (1978) [JETP Lett. 27, 123 (1978)].

<sup>15</sup>D. N. Kozlov, Diploma Project, MFTI, Moscow, 1977; Abstract of Candidate Thesis, MFTI, Moscow, 1980.

<sup>16</sup>A. D. May, M. A. Hennesian, and R. L. Byer, Can. J. Phys. 56, 248 (1978).

<sup>17</sup>N. D. Orlova and L. A. Platonova, Pis'ma Zh. Eksp. Teor. Fiz. 31, 10

- (1980) [JETP Lett. **31**, 8 (1980)].
- <sup>18</sup>S. A. Akhmanov and N. I. Koroteev, *Metody nelineinoi optiki v spektroskopii resseyaniya sveta (Methods of Nonlinear Optics in the Spectroscopy of Scattered Light)*, Nauka, Moscow 1981.
- <sup>19</sup>E. D. Bulatov, D. N. Kozlov, E. A. Otlivanchik, *et al*, *Kvantovaya Elektron.* **7**, 1294 (1980) [Sov. J. Quantum Electron. **10**, 740 (1980)].
- <sup>20</sup>D. N. Kozlov, A. M. Prokhorov, and V. V. Smirnov, *Mol. Spectr.* **77**, 21 (1979).
- <sup>21</sup>G. Ya. Zueva, D. N. Kozlov, P. V. Nickles, *et al.*, *Opt. Comm.* **35**, 218 (1980).
- <sup>22</sup>L. Ya. Baranov, B. I. Zhilinskii, D. N. Kozlov, *et al.*, *Zh. Eksp. Teor. Fiz.* **78**, 46 (1980) [Sov. Phys. JETP **51**, 22 (1980)].
- <sup>23</sup>G. Pierre, G. P. Champion, D. N. Kozlov, and V. V. Smirnov, *J. Phys.* **43**, 1429 (1982).
- <sup>24</sup>P. Hess, A. H. Kung, and C. B. Moore, *J. Chem. Phys.* **72**, 5525 (1980).
- <sup>25</sup>J. E. Lolck and A. G. Robiette, *Chem. Phys. Lett.* **64**, 195 (1979).
- <sup>26</sup>A. D. May, J. C. Stryland, and H. J. Welsh, *J. Chem. Phys.* **30**, 1099 (1959).
- <sup>27</sup>M. J. Clouter, H. Kieft, and R. K. Jain, *J. Chem. Phys.* **73**, 673 (1980).

Translated by S. Chomet